博士学位論文

慢性運動に関連する筋骨連関における peripheral myelin protein 22 の役割

近畿大学大学院
医学研究科医学系専攻
川口美紅

川口美紅

Doctoral Dissertation

Role of peripheral myelin protein 22 in chronic exercise-induced interactions of muscle and bone in mice

October 2022

Major in Medical Sciences
Kindai University Graduate School of Medical Sciences

Miku Kawaguchi

課博・論博

同　意　書

2022 年 10 月 24 日

近畿大学大学院
医学研究科長　殿

共著者　河尻直之　印　　共著者　高藤義正　印

共著者　木下優子　印　　共著者　高田雄斗　印

共著者　水上優哉　印　　共著者　大平宇志　印

共著者　梶博史　印　　共著者　　印

共著者　　印　　共著者　　印

論文題目

Role of peripheral myelin protein 22 in chronic exercise-induced interactions of muscle and bone in mice

下記の博士論文提出者が、標記論文を貴学医学博士の学位論文（主論文）として使用することに同意いたします。

また、標記論文を再び学位論文として使用しないことを誓約いたします。

記

1．博士論文提出者氏名　　川口　美紅

2．専攻分野　　医学系　　分子生体制御学

課博・論博

同　意　書

2022年 10月 24日

近畿大学大学院
医学研究科長　殿

共著者 村谷匡史 ㊞　　共著者 ＿＿＿＿＿＿＿＿ ㊞

共著者 ＿＿＿＿＿＿＿＿ ㊞　　共著者 ＿＿＿＿＿＿＿＿ ㊞

共著者 ＿＿＿＿＿＿＿＿ ㊞　　共著者 ＿＿＿＿＿＿＿＿ ㊞

共著者 ＿＿＿＿＿＿＿＿ ㊞　　共著者 ＿＿＿＿＿＿＿＿ ㊞

共著者 ＿＿＿＿＿＿＿＿ ㊞　　共著者 ＿＿＿＿＿＿＿＿ ㊞

論文題目

Role of peripheral myelin protein 22 in chronic exercise-induced interactions of muscle and bone in mice

下記の博士論文提出者が、標記論文を貴学医学博士の学位論文（主論文）として使用することに同意いたします。

また、標記論文を再び学位論文として使用しないことを誓約いたします。

記

1．博士論文提出者氏名　　川口　美紅

2．専攻分野　　医学系　　分子生体制御学

課博・論博

同　意　書

2022年　10月　24日

近畿大学大学院
医学研究科長　殿

共著者　石田昌義　印　　共著者　＿＿＿＿＿＿＿＿　印

共著者　＿＿＿＿＿＿＿＿　印　　共著者　＿＿＿＿＿＿＿＿　印

共著者　＿＿＿＿＿＿＿＿　印　　共著者　＿＿＿＿＿＿＿＿　印

共著者　＿＿＿＿＿＿＿＿　印　　共著者　＿＿＿＿＿＿＿＿　印

共著者　＿＿＿＿＿＿＿＿　印　　共著者　＿＿＿＿＿＿＿＿　印

論文題目

Role of peripheral myelin protein 22 in chronic exercise-induced interactions of muscle and bone in mice

下記の博士論文提出者が、標記論文を貴学医学博士の学位論文（主論文）として使用することに同意いたします。

また、標記論文を再び学位論文として使用しないことを誓約いたします。

記

1．博士論文提出者氏名　　川口　美紅

2．専攻分野　　医学系　　分子生体制御学

Role of peripheral myelin protein 22 in chronic exercise-induced interactions of muscle and bone in mice

Miku Kawaguchi[1], Naoyuki Kawao[1], Masafumi Muratani[2], Yoshimasa Takafuji[1], Masayoshi Ishida[1], Yuko Kinoshita[1], Yuto Takada[1], Yuya Mizukami[1], Takashi Ohira[1], Hiroshi Kaji[1,*]

[1]Department of Physiology and Regenerative Medicine, Kindai University Faculty of Medicine, Osakasayama, 377-2 Ohnohigashi, Osakasayama, Osaka 589-8511, Japan, [2]Department of Genome Biology, University of Tsukuba, Tsukuba, Japan.

***Corresponding author:** Hiroshi Kaji, M. D., Department of Physiology and Regenerative Medicine, Kindai University Faculty of Medicine, 377-2 Ohnohigashi, Osakasayama, Osaka 589-8511, Japan.
E-mail: hkaji@med.kindai.ac.jp

Financial Support: This study was partly supported by a grant from All-Kindai University support project against COVID-19 to N.K., a grant from Grant-in-Aid for Scientific Research (C: 20K09514) to HK and (C: 19K07310) to NK and a Grant-in-Aid for Scientific Research on Innovative Areas (grant number 15H05935, "Living in Space") from the Ministry of Education, Culture, Sports, Science, and Technology of Japan to HK.

Disclosure: The authors declare that they have no conflicts of interest with the contents of this article.

Data availability: The data sets used and/or analyzed during the current study are available from the corresponding author on reasonable request.

Abstract

Exercise is important for the prevention and treatment of sarcopenia and osteoporosis. Although the interactions between skeletal muscles and bone have recently been reported, the myokines linking muscle to bone during exercise remain unknown. We previously revealed that chronic exercise using treadmill running blunts ovariectomy-induced osteopenia in mice. We herein performed an RNA sequence analysis of the gastrocnemius and soleus muscles of male mice with or without chronic exercise to identify the myokines responsible for the effects of chronic exercise on the muscle/bone relationship. We extracted peripheral myelin protein 22 (PMP22) as a humoral factor that was putatively induced by chronic exercise in the soleus and gastrocnemius muscles of mice from the RNA sequence analysis. Chronic exercise significantly enhanced the expression of PMP22 in the gastrocnemius and soleus muscles of female mice. PMP22 suppressed macrophage-colony stimulating factor and receptor activator factor κB ligand-induced increases in the expression of osteoclast-related genes and osteoclast formation from mouse bone marrow cells. Moreover, PMP22 significantly inhibited osteoblast differentiation, alkaline phosphatase activity and mineralization in mouse osteoblast cultures; however, the overexpression of PMP22 did not affect muscle phenotypes in mouse muscle C2C12 cells. A simple regression analysis revealed that PMP22 mRNA levels in the gastrocnemius and soleus muscles were positively related to cortical bone mineral density at the femurs of mice with or without chronic exercise. In conclusion, we identified PMP22 as a novel myokine induced by chronic exercise in mice. We first showed that PMP22 suppresses osteoclast formation and the osteoblast phenotype *in vitro*.

Keywords: PMP22, Exercise, Bone, Muscle

1. Introduction

Exercise therapy is important for the prevention and treatment of sarcopenia and osteoporosis (Smith, 2018; Wallace and Cumming, 2000). Clinical evidence suggests that exercise effectively increases bone mineral density (BMD) in postmenopausal osteoporosis (Kemmler et al., 2020). Regarding the effects of mechanical loading on bone formation and resorption, mechanical stress has been shown to suppress bone resorption through its sensing by osteocytes, and sclerostin, a Wnt signal inhibitor, partly participates in this mechanism (Baron and Kneissel, 2013). The ion channels, connexin 43 and Piezo 1 may be included in mechanosensors in bone cells (Batra et al., 2012; Gilchrist et al., 2019; Wang et al., 2020). However, the mechanisms by which exercise regulates bone remodeling have remained clear.

Since sarcopenia has been related to osteoporosis, which raised the notion of the interactions between skeletal muscles and bone (Kaji, 2013; Kawao and Kaji, 2015). Genetic factors, mechanical stress, nutrition, inflammation, cachexia and endocrine factors simultaneously influence muscle and bone (Kawao and Kaji, 2015). Recent findings proposed significant roles for myokines, muscle-derived humoral factors, in the interactions between muscle and bone (Kaji, 2016; Schnyder and Handschin, 2015). Myokines participate in metabolic regulation during exercise. Myostatin, irisin, follistatin, insulin-like growth factor-1, fibroblast growth factor-2, interlekin-6 and osteoglycin have been identified as myokines that affect bone (Kaji, 2016). Irisin is an important myokine that plays roles in the muscle/bone relationship. It was shown to be released from skeletal muscles into the circulation with acute exercise (Kaji, 2016). Furthermore, we recently reported the involvement of irisin in unloading-induced osteopenia in mice (Kawao et al., 2018b). Moreover, chronic exercise enhanced the expression of irisin in the

skeletal muscles of mice (Kawao et al., 2021). Therefore, irisin has potential as a biomarker for the evaluation of exercise and also as a target of drug development for osteoporosis. We recently suggested the potential involvement of several novel myokines, such as follistatin, olfactomedin1 and Dkk2, as well as muscle-derived extracellular vesicles in muscle wasting and osteopenia induced by mechanical unloading or gravity changes (Kawao et al., 2020a; Kawao et al., 2018a; Shimoide et al., 2020; Takafuji et al., 2020; Takafuji et al., 2021). However, the myokines that play significant roles in the interactions between muscle and bone during exercise remain unknown.

To identify the crucial myokines responsible for the effects of chronic exercise on muscle and bone in mice, we recently performed experiments using treadmill exercise with moderate intensity (aerobic exercise) for 8 weeks (Kawao et al., 2021). The findings obtained revealed that chronic exercise ameliorated ovariectomy-induced decreases in the BMD of trabecular and cortical bones at the femurs and elevated the expression of irisin in the gastrocnemius and soleus muscles. As the next step, we herein performed a comprehensive RNA sequence (RNA-seq) analysis of the gastrocnemius and soleus muscles of mice with or without chronic exercise.

2. Materials and Methods

2.1 Materials

Recombinant PMP22 was purchased from Cloud-Clone Corp. (Wuhan, China). Anti-PMP22 antibody was from Sigma (Cat. No. SAB4502217, St. Louis, MO, USA). Anti-phosphorylated p38 (Cat. No. 9211), anti-p38 (Cat. No. 9212), anti-phosphorylated extracellular signal-regulated kinase 1/2 (ERK1/2, Cat. No. 9101), anti-ERK1/2 (Cat. No. 9102), anti-

phosphorylated p65 (Cat. No. 3033), anti-p65 (Cat. No., 8242), anti-phosphorylated Akt (Cat. No. 4060), anti-Akt (Cat. No. 4691), anti-phosphorylated p70S6 kinase (Cat. No. 9234), anti-p70S6 kinase (Cat. No. 2708) and anti-glyceraldehyde-3-phosphate dehydrogenase (GAPDH, Cat. No. 5174) antibodies were from Cell Signaling Technology (Danvers, MA, USA).

2.2 Animals

C57BL/6J mice were obtained from CLEA Japan (Tokyo, Japan). Animal experiments were performed according to the guidelines of the National Institutes of Health and the institutional rules for the use and care of laboratory animals at Kindai University. All animal experiments were approved by the Experimental Animal Welfare Committee of Kindai University (Permit number: KAME-27-029).

2.3 Exercise protocol

Moderate intensity continuous training was performed on a treadmill (TMS-4, Melquest, Toyama, Japan) 5 days/week for 8 weeks in accordance with a previously described exercise protocol (Wang et al., 2017). Exercise was started with a warm-up at 5 m/min, followed by treadmill exercise consisting of continuous running (65-70% VO_{2max}). For the experiments with treadmill exercise, eight-week-old female mice performed moderate intensity exercise protocol with treadmill exercise for 8 weeks, as previously described (Kawao et al., 2021).

2.4 Sciatic-neurectomized (SNX) mice

SNX or sham surgery was performed on 7-week-old C57BL/6J male mice, as previously

described (Kawao et al., 2018b). Mice were euthanized with excess isoflurane 4 weeks after SNX surgery and the gastrocnemius and soleus muscles were collected.

2.5 RNA-seq

We performed an RNA-seq analysis of the gastrocnemius and soleus muscles of 8-week-old male mice with moderate intensity continuous training on a treadmill 5 days/week for 8 weeks, as previously described (Kawao et al., 2020b). Each library was sequenced using Illumina (2×36-bp paired-end reads) with NextSeq500 High Output Kit v2 (Illumina, San Diego, CA, USA). Reads were mapped to the mm10 mouse reference genome and quantified for 49,585 annotated genes. Reads per kilobase of transcript per million mapped reads values were normalized by the quantile method.

2.6 Real-time polymerase chain reaction (PCR)

Real-time PCR was performed using the StepOnePlus Real-Time PCR system (Applied Biosystems) with the Fast SYBR Green Master mix (Applied Biosystems), as previously described (Kawao et al., 2018b). Primer sequences are shown in Table S1.

2.7 Osteoclast formation

Osteoclast formation was induced in mouse bone marrow cells as previously described (Kawao et al., 2018b). Osteoclasts were detected using a tartrate-resistant acid phosphatase (TRAP) staining kit (Wako Pure Chemicals, Osaka, Japan), and the numbers of TRAP-positive multinucleated cells with three and more nuclei were counted in each well.

Table S1 Primers used for real-time PCR experiments.

Gene		Primer sequence
PMP22	Forward	5'-ATGGACACACGACTGATCTCT-3'
	Reverse	5'-CAGCCATTCGCTCACTGATGA-3'
NFATc1	Forward	5'-CAAGTCTCACCACAGGGCTCACTA-3'
	Reverse	5'-GCGTGAGAGGTTCATTCTCCAAGT-3'
TRAP	Forward	5'-CAGCTGTCCTGGCTCAAAA-3'
	Reverse	5'-ACATAGCCCACACCGTTCTC-3'
Cathepsin K	Forward	5'-GAGGGCCAACTCAAGAAGAA-3'
	Reverse	5'-GCCGTGGCGTTATACATACA-3'
DC-SATMP	Forward	5'-TATCTGCTGTATCGGCTCAT-3'
	Reverse	5'-AGAATAATACTGAGAGGAACCCA-3'
MafB	Forward	5'-GCAACGGTAGTGTGGAGGAC-3'
	Reverse	5'-ACCTCGTCCTTGGTGAAGC-3'
IRF-8	Forward	5'-AGACCATGTTCCGTATCCCCT-3'
	Reverse	5'-CACAGCGTAACCTCGTCTTCC-3'
RANKL	Forward	5'-CACAGCGCTTCTCAGGAGCT-3'
	Reverse	5'-CATCCAACCATGAGCCTTCC-3'
OPG	Forward	5'-AGTCCGTGAAGCAGGAGT-3'
	Reverse	5'-CCATCTGGACATTTTTTGCAAA-3'
PGC1β	Forward	5'-CCTCATGCTGGCCTTGTCA-3'
	Reverse	5'-TGGCTTGTATGGAGGTGTGG-3'
Runx2	Forward	5'-AAATGCCTCCGCTGTTATGAA-3'
	Reverse	5'-GCTCCGGCCCACAAATCT-3'
Osterix	Forward	5'-AGCGACCACTTGAGCAAACAT-3'
	Reverse	5'-GCGGCTGATTGGCTTCTTCT-3'
ALP	Forward	5'-ATCTTTGGTCTGGCTCCCATG-3'
	Reverse	5'-TTTCCCGTTCACCGTCCAC-3'
Osteocalcin	Forward	5'-CCTGAGTCTGACAAAGCCTTCA-3'
	Reverse	5'-GCCGGAGTCTGTTCACTACCTT-3'
MyoD	Forward	5'-AGCACTACAGTG GCGACTCAG-3'
	Reverse	5'-AGGCGGTGTCGTAGCCAT TC-3'
Myogenin	Forward	5'-GCTGCCTAAAGTGGAGAT CCT-3'
	Reverse	5'-GCGCTGTGGGAGTTGCAT-3'
MHC-I	Forward	5'-GCCAACTATGCT GGAGCTGATGCCC-3'
	Reverse	5'-GGTGCGTGGAGCGCAAGTTTGTCATAAG-3'
MHC-IIb	Forward	5'-CGAAGGCGGAGCTACGGTCA-3'
	Reverse	5'-CGG CAGCCACTTGTAGGGGT-3'
Atrogin-1	Forward	5'-GTCGCAGCCAAGAAGAGAAAGA-3'
	Reverse	5'-TGCTATCAGCTCCAACAGCCTT-3'
MuRF1	Forward	5'-TAACTGCATCTCCATGCTGGTG-3'
	Reverse	5'-TGGCGTAGAGGGTGTCAAACTT-3'
18S rRNA	Forward	5'-CGGCTACCACATCCAAGGAA-3'
	Reverse	5'-GCTGGAATTACCGCGGCT-3'

PMP22, peripheral myelin protein 22; NFATc1, nuclear factor of activated T cells; TRAP, tartrate-resistant acid phosphatase; DC-STAMP, dendrocyte expressed seven transmembrane protein; IRF-8, interferon regulatory factor 8; OPG, osteoprotegerin; PGC1β, peroxisome proliferator-activated receptor gamma coactivator 1-β; ALP, alkaline phosphatase; MHC-I, Myosin heavy chain-I; MHC-IIb, Myosin heavy chain-IIb.

2.8 Oxygen consumption measurement

To measure the oxygen consumption rate (OCR), mouse bone marrow cells were analyzed using an XF96 Extracellular Flux Analyzer with a Mito Stress kit (Seahorse Bioscience, North Billerica, MA, USA) as previously described (Takafuji et al., 2020). Mouse bone marrow cells were seeded in XF96 cell culture microplates (0.5×10^4 cells/well) and cultured with 50 ng/ml macrophage colony-stimulating factor (M-CSF) for 3 days and 50 ng/ml M-CSF and 75 ng/ml receptor activator of nuclear factor κB ligand (RANKL) for a further 4 days.

Culture medium was changed to Agilent Seahorse XF Base Medium supplemented with glucose (10 mM), sodium pyruvate (1 mM) and L-glutamine (2 mM) 1 h before measurements. Basal OCR and OCR after injections of 1 μM oligomycin, 1 μM carbonyl cyanide 4-(trifluoromethoxy) phenylhydrazone (FCCP), and 0.5 μM rotenone/0.5 μM antimycin A for three measurement cycles at each step were analyzed.

2.9 Western blot

A Western blot analysis was performed with anti-phosphorylated p38, anti-p38, anti-phosphorylated ERK1/2, anti-ERK1/2, anti-phosphorylated p65, anti-p65, anti-phosphorylated Akt, anti-Akt, anti-phosphorylated p70 S6 kinase, anti-p70 S6 kinase, anti-PMP22 and anti-GAPDH antibodies as previously described (Shimoide et al., 2020).

2.10 Preparation of primary osteoblasts

Primary osteoblasts were collected from the calvaria of newborn C57BL/6J mice as previously described (Kawao et al., 2013).

2.11 Alkaline phosphatase (ALP) activity

Primary mouse osteoblasts were cultured in 24-well plates until confluent. ALP activity was analyzed using the Lab assay ALP kit (Wako Pure Chemicals) as previously described (Kawao et al., 2013).

2.12 Mineralization of primary osteoblasts

To examine the effects of PMP22 on mineralization, primary mouse osteoblasts with or without 10^{-8} M of the PMP22 recombinant protein were cultured for 3 weeks in Minimum Essential Medium Alpha Modification (αMEM) with 10% FBS and 1% penicillin/streptomycin. To detect mineralization levels, cells were fixed with 4% formaldehyde and stained with Alizarin Red.

2.13 Culture of C2C12 cells

Mouse myoblastic C2C12 cells were obtained from ATCC (Manassas, VA, USA) and cultured in high glucose Dulbecco's Modified Eagle's Medium (DMEM; Wako) with 10% FBS and 1% penicillin/streptomycin. Medium was changed twice a week.

2.14 DNA construction

The coding region of murine PMP22 was amplified by PCR with the KAPA HiFi DNA Polymerase enzyme (KAPA Biosystems, Wilmington, MA, USA) using cDNA from the mouse neonatal brain as a template and primers (5'-ATATAGCTGACATGCTCCTACTCTTGTTGGG-3' as the forward primer and 5'-ATATACTCGAGTCATTCGCGTTTCCGCAGGA-3' as the reverse primer). PMP22 cDNA was inserted into the mammalian expression vector, pcDNA3.1(+) (Invitrogen, Thermo Fisher Scientific) and the sequence was verified.

2.15 Transient transfection

Regarding transient transfection, the PMP22 expression vector was transfected into C2C12 cells using the jetPRIME reagent (Polyplus-transfection SA, Illkirch, France) according to the manufacturer's protocol. Transfected C2C12 cells were cultured in 2% horse serum for 5 days. Transfection efficiency was confirmed with qRT-PCR for PMP22 for each experiment.

2.16 Quantitative computed tomography (QCT) analysis

A QCT analysis was performed according to our previous study (Tamura et al., 2014). The femurs of mice were scanned using an X-ray CT system (Latheta LCT-200; Hitachi Aloka Medical, Tokyo, Japan). CT images were acquired using 24-μm isotropic voxel sizes for the analysis of the femur. Regions of interest were defined as 1680 μm (70 slices) segments from 96 μm proximal to the end of the distal growth plate towards the diaphysis of the femur for the assessment of trabecular BMD. Regions of interest were defined as 2160 μm (90 slices)

segments of the mid-diaphysis of the femur for the assessment of cortical BMD. These bone parameters were analyzed using LaTheta software (version 3.41).

2.17 Statistical analysis

Data are expressed as the mean ± the standard error of the mean (SEM). Results represent experiments independently performed at least 3 times. The significance of differences was evaluated using the Mann-Whitney *U* test for comparisons of two groups. A one- or two-way analysis of variance followed by Dunnett's test or the Tukey-Kramer test was performed for multiple comparisons. The significance level was set at $P < 0.05$. All statistical analyses were conducted using GraphPad PRISM 7.00 software.

3. Results

3.1 RNA-seq analysis of soleus and gastrocnemius muscles

We performed an RNA-seq analysis to identify the factors induced by chronic exercise in the soleus and gastrocnemius muscles of male mice. We extracted 16 RNAs with a ratio of expression of RNAs induced by chronic exercise that was greater than 1.5 fold in both the soleus and gastrocnemius muscles of mice (Table 1). We were interested in some novel circulating myokines, which might link muscle to bone by affecting bone, in the effects of chronic exercise on bone. Among the extracted RNAs, we focused on PMP22 because it may be a humoral factor that is putatively induced by chronic exercise in both the soleus and gastrocnemius muscles of mice. We examined the expression of PMP22 in the soleus and gastrocnemius muscles of female mice with or without chronic exercise. Chronic exercise significantly enhanced the

mRNA expression and protein levels of PMP22 in both the gastrocnemius and soleus muscles of mice. PMP22 mRNA levels were significantly higher in the soleus muscles than in the gastrocnemius muscles (Fig. 1A, 1B). We then examined the expression of PMP22 in various organs, such as the femurs, white adipose tissue (WAT), kidneys and liver. Chronic exercise significantly increased PMP22 mRNA levels in the skeletal muscles, but not in the femurs, WAT, kidneys or liver (Fig. 1C). Chronic exercise partly influences skeletal muscles through an increase in mechanical stress, and mechanical unloading might reduce PMP22 expression in contrast to the effects of chronic exercise on PMP22 expression in muscles of mice. We then used bilateral SNX mice to investigate the effects of mechanical unloading on PMP22 expression in the skeletal muscles of mice. SNX significantly reduced PMP22 mRNA levels in the soleus, but not gastrocnemius, muscles of mice (Fig. 1D).

Table 1 Gene transcripts in the soleus and gastrocnemius muscles of mice after chronic exercise

Gene	Gene accession number	Fold change	
		Gastrocnemius muscle (≥1.50)	Soleus muscle (≥1.50)
Rny1	NR_004419	3.24	2.43
Csrp3	NM_013808	3.17	3.94
Rny3	NR_024202	2.75	3.91
Gm24187	XM_002031117	2.70	1.67
Klf4	NM_010637	2.67	1.86
2310075C17Rik	NR_131053	2.52	2.01
Otud1	NM_027715	2.42	2.03
Ankrd2	NM_020033	2.15	4.64
Gm24305	XR_004937873	2.11	2.32
Rnu12	NR_004432	2.11	2.55
Mbp	NM_001025251	1.80	2.96
Pmp22	NM_001302255	1.78	2.30
Mpz	NM_001315499	1.78	3.19
Gm8797	-	1.64	2.44
Ckmt2	NM_198415	1.56	2.29
Hspb7	NM_013868	1.51	2.21

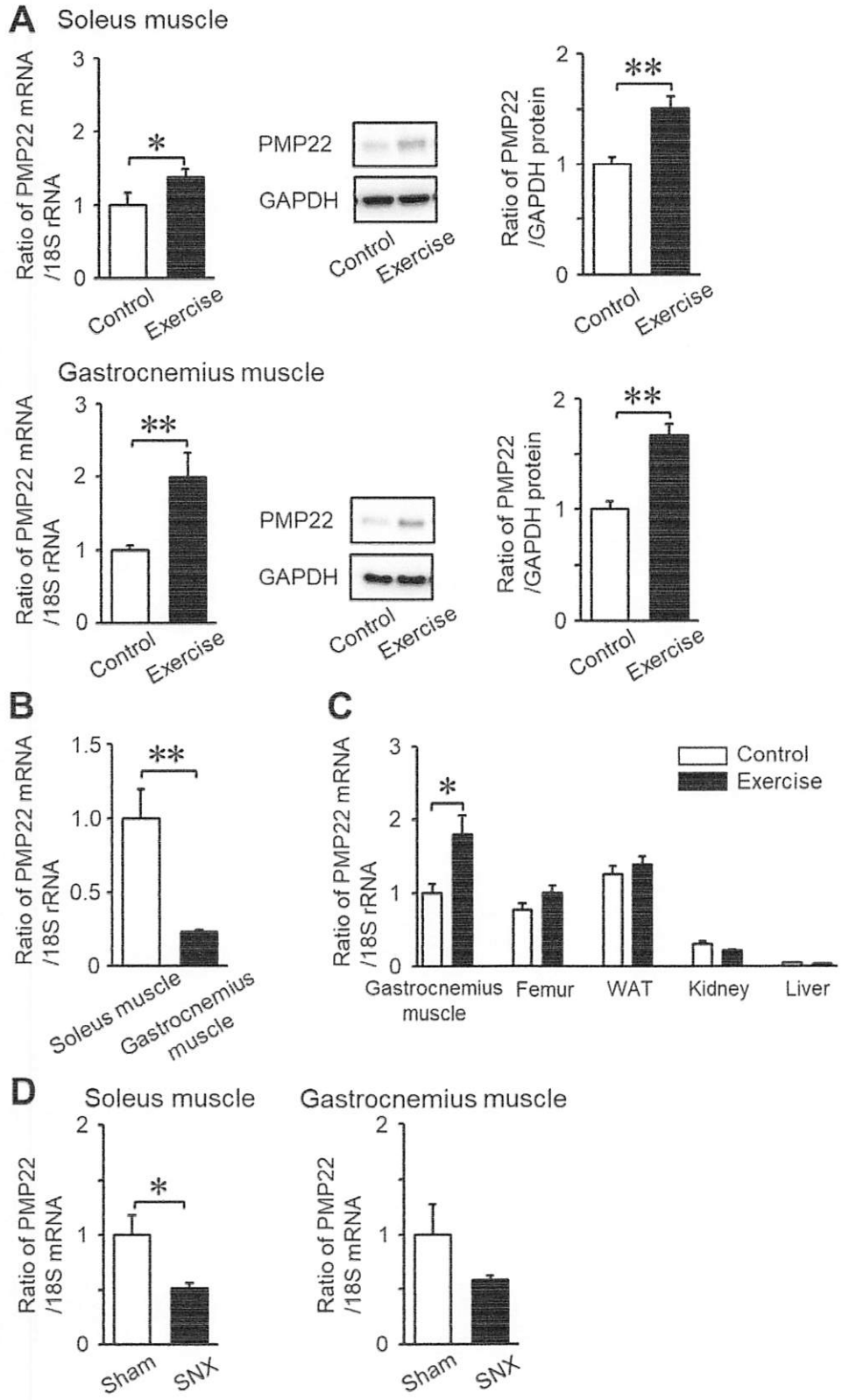

Figure 1 Effects of chronic exercise on PMP22 expression in mice. (A, B, C) Total RNA was extracted from the soleus and gastrocnemius muscles, femurs, white adipose tissues (WAT), kidneys and liver of mice 8 weeks after the initiation of treadmill exercise. A real-time PCR analysis of PMP22 and 18S rRNA was performed. Data represent the mean ± SEM. n = 10 mice in each group (A, soleus muscle) and 8 mice in each group (A, gastrocnemius muscle). n = 8 mice in each group (B, C). For Western blot analysis, total protein

was extracted from the soleus and gastrocnemius muscles of mice 8 weeks after the initiation of treadmill exercise. Western blot and the quantitation of blot were performed as described in Materials and Methods. Data represent the mean ± SEM (n = 5 mice in each group). (D) Total RNA was extracted from the soleus and gastrocnemius muscles of control and bilateral sciatic-neurectomized (SNX) mice 4 weeks after SNX surgery. A real-time PCR analysis of PMP22 and 18S rRNA was performed. Data represent the mean ± SEM (n = 6 mice in each group). *P < 0.05, **P < 0.01 (Mann-Whitney *U* test).

3.2 Effects of PMP22 on bone resorption

We examined the effects of PMP22 on osteoclast formation in mice *in vitro*. PMP22 suppressed the M-CSF and RANKL-induced osteoclast formation from mouse bone marrow cells in a dose-dependent manner (Fig. 2A). Moreover, PMP22 significantly decreased M-CSF and RANKL-induced increases in the mRNA levels of NFATc1, TRAP, cathepsin K and DC-STAMP in bone marrow cells, but inhibited M-CSF and RANKL-induced reductions in the mRNA levels of MafB and IRF-8, which are NFATc1-related genes (Fig. 2B). It is well known that RANKL, expressed in osteoblasts, stromal cells or osteocytes, mediates the regulation of numerous factors on bone resorption (Udagawa et al., 2021). We therefore examined the effects of PMP22 on RANKL expression in mouse osteoblasts. PMP22 significantly increased the mRNA levels of RANKL and the ratio of RANKL/OPG mRNA in mouse primary osteoblasts, but did not affect OPG mRNA levels (Fig. 2C).

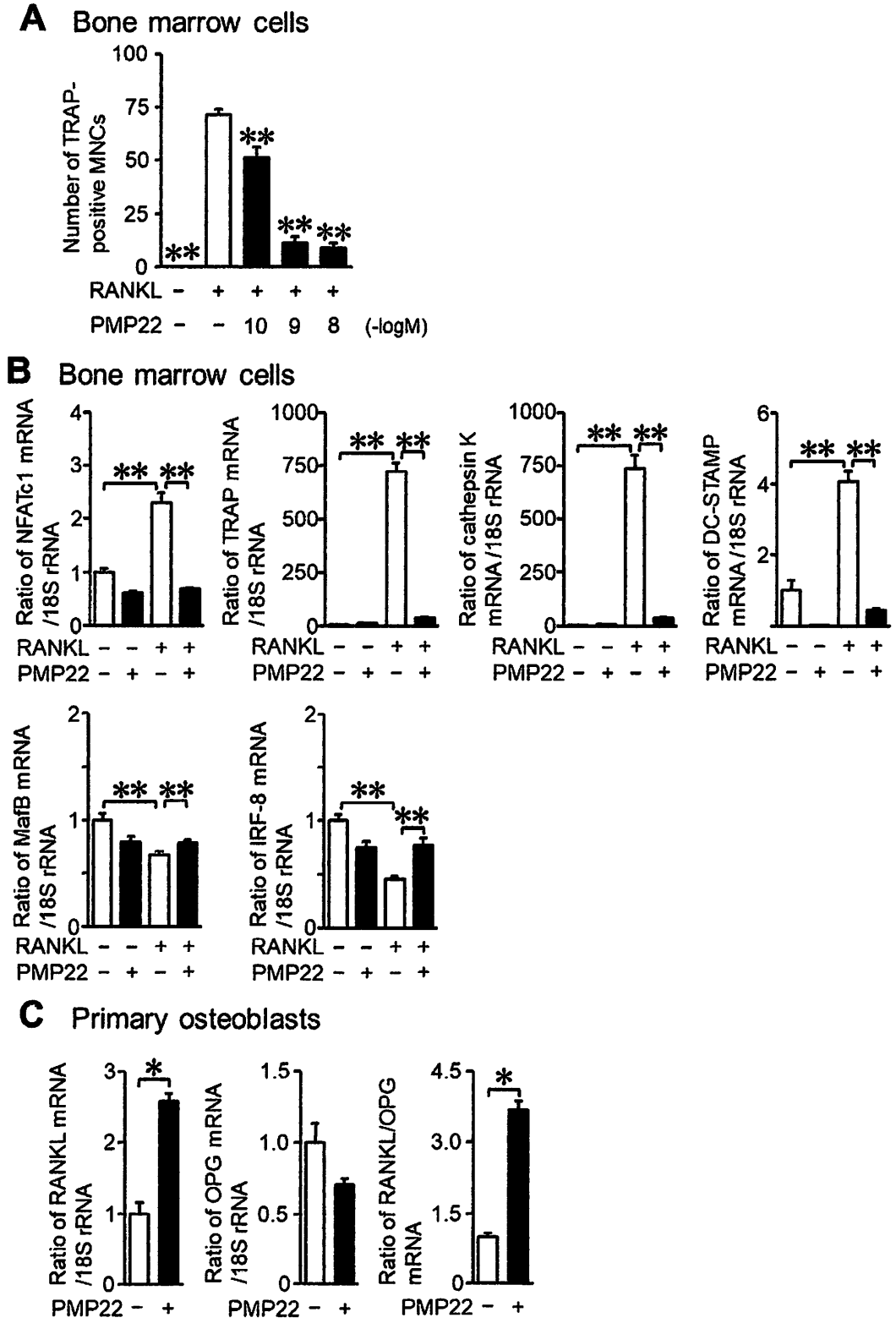

Figure 2 Effects of PMP22 on osteoclast formation in mouse bone marrow cells. (A) Mouse bone marrow cells were pre-cultured with 50 ng/ml M-CSF for 3 days, and further cultured with 50 ng/ml M-CSF and 75 ng/ml RANKL in the presence or absence of recombinant PMP22 at the indicated concentration for an additional 4 days. Cells were stained with TRAP staining, and the number of TRAP-positive multinucleated cells (MNCs) was counted in each well. Data represent the mean ± SEM (n = 5 in each group). **P < 0.01 versus the RANKL-treated group (Dunnett's test). (B) Mouse bone marrow cells were pre-cultured with 50 ng/ml M-CSF for 3 days, and further cultured with 50 ng/ml M-CSF and 75 ng/ml RANKL in the presence

or absence of 10^{-8} M of recombinant PMP22 for an additional 4 days. A real-time PCR analysis of NFATc1, TRAP, cathepsin K, DC-STAMP, MafB, IRF-8 and 18S rRNA was performed. Data represent the mean ± SEM (n = 5 in each group). **P < 0.01 (Tukey-Kramer test). (C) Mouse osteoblasts were cultured with or without 10^{-8} M of recombinant PMP22 for 24 h. A real-time PCR analysis of RANKL, OPG and 18S rRNA was performed. Data represent the mean ± SEM (n = 5 in each group). *P < 0.05 (Mann-Whitney *U* test).

3.3 Effects of PMP22 on bone marrow cells

A previous study indicated that mitochondrial energy metabolism is increased during osteoclast differentiation in mice, and the energy required for osteoclast differentiation mainly derives from mitochondrial oxidative metabolism (Lemma et al., 2016). We therefore examined the effects of PMP22 on mitochondrial biogenesis to elucidate the mechanisms by which PMP22 suppresses osteoclast differentiation in mouse bone marrow cells. As shown in Fig. 3A, PMP22 significantly decreased OCR in the bone marrow cells cultured with M-CSF and RANKL for 4 days. Moreover, PMP22 significantly reduced the mRNA levels of PGC1β (Fig. 3B), a key regulator of mitochondrial biogenesis (Ishii et al., 2009; Zeng et al., 2015). In addition, we examined the effects of PMP22 on mitogen-activated protein kinase (MAPK) and NF-κB pathway, crucial pathways for osteoclast formation (Koga et al., 2019), in mouse bone marrow cells. PMP22 significantly enhanced the phosphorylation of p38 MAPK in mouse bone marrow cells, but inhibited that of ERK1/2 (Fig. 3C). We then examined the effects of PMP22 on the NF-κB pathway induced by RANKL in mouse bone marrow cells. PMP22 significantly reduced the phosphorylation of the NF-κB p65 subunit in the presence of RANKL in bone marrow cells (Fig. 3D).

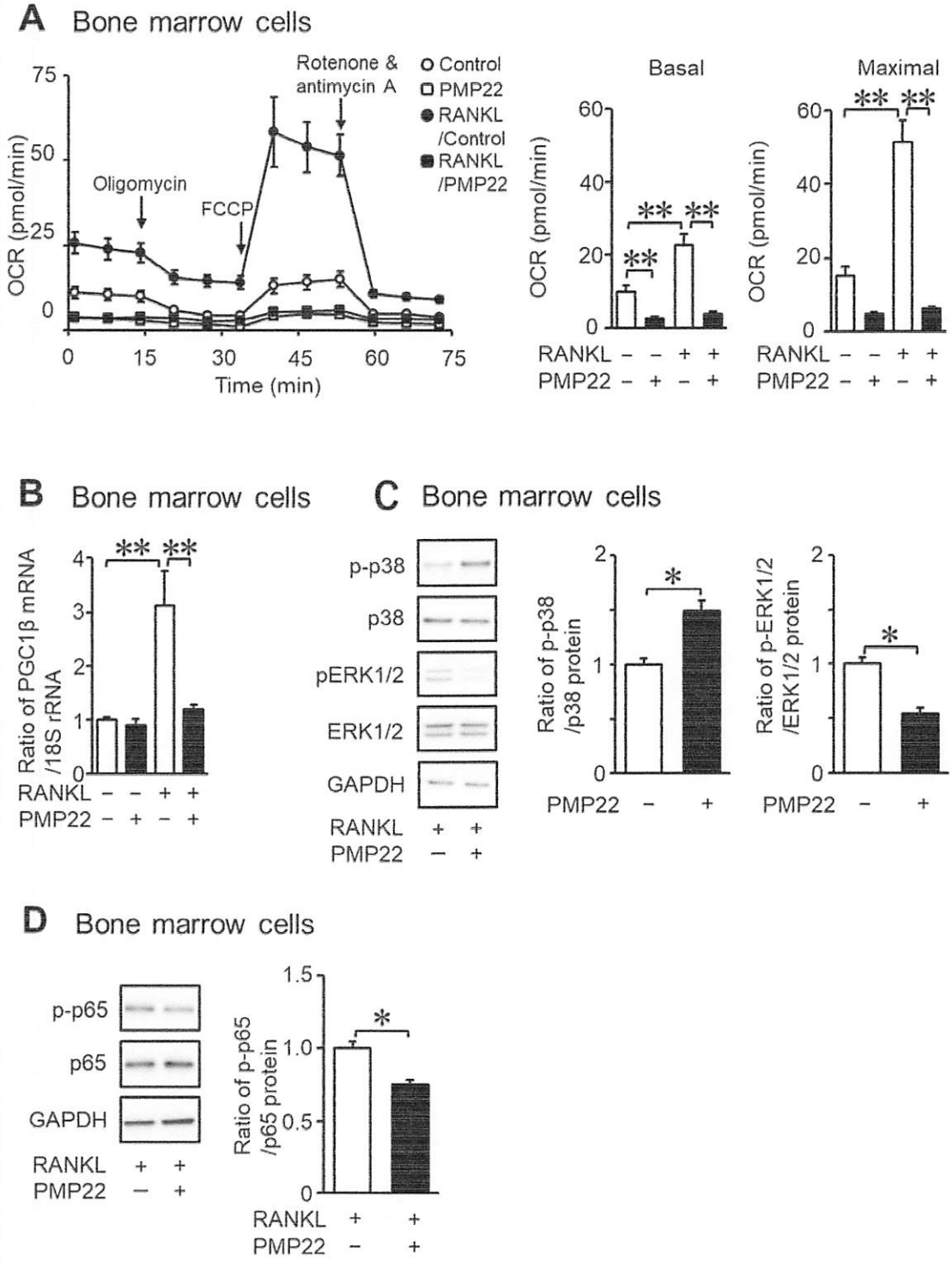

Figure 3 Effects of PMP22 on mitochondrial biogenesis and MAPK and NF-κB pathways in mouse bone marrow cells. Mouse bone marrow cells were pre-cultured with 50 ng/ml M-CSF for 3 days, and further cultured in 50 ng/ml M-CSF and 75 ng/ml RANKL in the presence or absence of 10^{-8} M of recombinant PMP22 for 4 days. (A) The OCR values of cells were analyzed with an XF96 Extracellular Flux Analyzer. Basal OCR (before the stimulation with oligomycin) and maximal OCR (after the stimulation with FCCP) were measured. Data represent the mean ± SEM (n = 10 in each group). (B) Total RNA was extracted from mouse bone marrow cells, and a real-time PCR analysis of PGC1β or 18S rRNA was performed. Data represent the mean ± SEM (n = 5 in each group). **P < 0.01 (Tukey-Kramer test). (C, D) Protein was extracted from mouse bone marrow cells and a Western blot analysis of phosphorylated p38 (p-p38), p38,

phosphorylated ERK1/2 (pERK1/2), ERK1/2, phosphorylated p65 (p-p65), p65 and GAPDH was performed. Images represent experiments independently performed at least four times. Data represent the mean ± SEM (n = 4 in each group). *P < 0.05 (Mann-Whitney *U* test).

3.4 Effects of PMP22 on osteoblasts

We investigated whether PMP22 affects mouse primary osteoblasts. The results obtained showed that PMP22 significantly suppressed the mRNA levels of Runx2, Osterix, ALP and osteocalcin, osteoblast differentiation-related genes, as well as ALP activity in mouse primary osteoblasts (Fig. 4A, 4B) Moreover, PMP22 significantly suppressed mineralization in mouse osteoblast cultures (Fig. 4C).

3.5 Effects of PMP22 on muscle cells

We investigated the effects of the overexpression of PMP22 on mouse muscle C2C12 cells to clarify whether PMP22 directly influences muscles. C2C12 cells differentiated into myotubes when treated with horse serum. The horse serum treatment for 5 days increased the mRNA levels of MyoD, myogenin, MHC-1 and MHC-IIb, which are muscle differentiation-related genes, in C2C12 cells (Fig. 5A). The transient overexpression of PMP22 did not affect horse serum-induced increases in the mRNA levels of MyoD, myogenin, MHC-I or MHC-IIb in these cells (Fig. 5A). Furthermore, the overexpression of PMP22 did not affect the mRNA levels of the muscle proteolytic factors, atrogin-1 and MuRF1, in cells treated with or without horse serum (Fig. 5B). Moreover, the overexpression of PMP22 did not affect the phosphorylation of Akt and p70 S6 kinase, which are muscle protein synthesis pathway, in C2C12 cells (Fig. 5C).

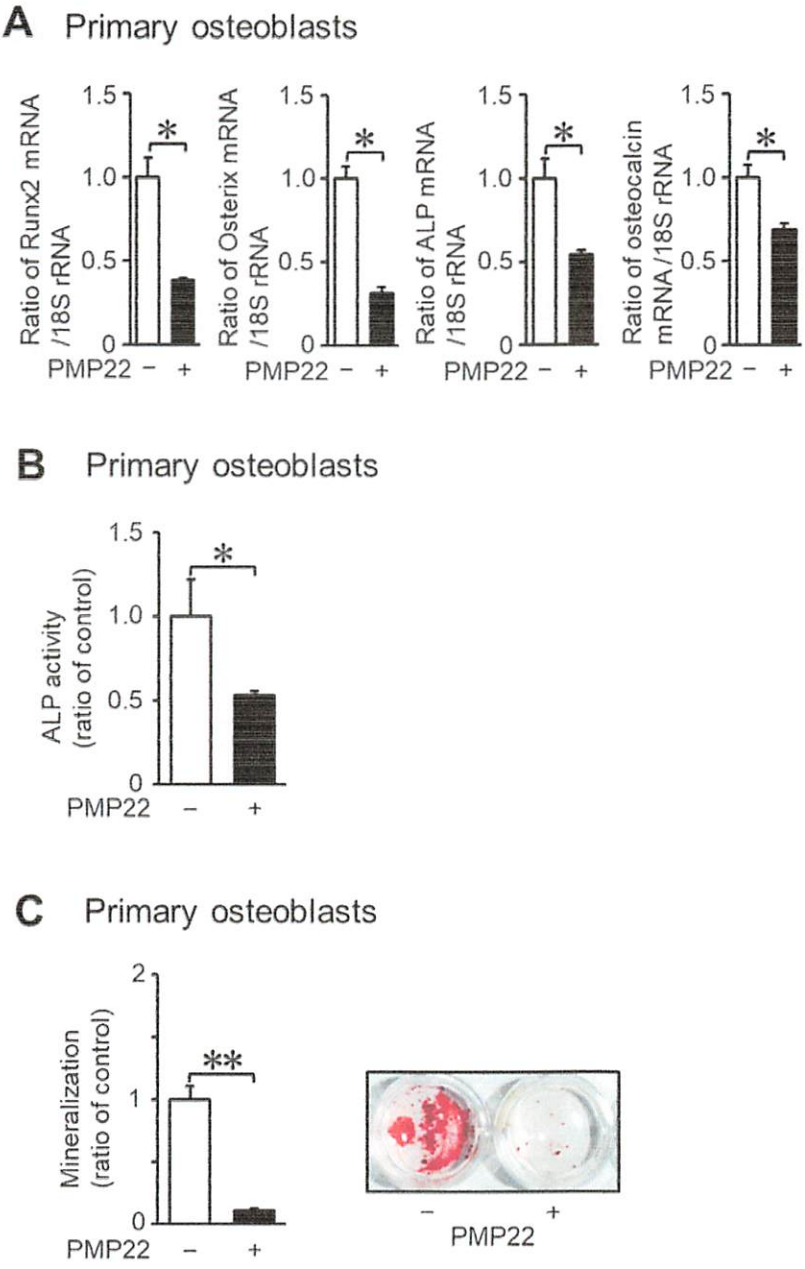

Figure 4 Effects of PMP22 on mouse primary osteoblasts. (A) Total RNA was extracted from mouse osteoblasts cultured with or without 10^{-8} M of PMP22 for 24 h, and a real-time PCR analysis of Runx2, Osterix, ALP, osteocalcin and GAPDH was performed. Data represent the mean ± SEM (n = 5 in each group). *P < 0.05 (Mann-Whitney *U* test). (B) ALP activity was measured in confluent mouse osteoblasts cultured with or without 10^{-8} M of PMP22 for 48 h. Data represent the mean ± SEM (n = 4 in each group). *P < 0.05 (Mann-Whitney *U* test). (C) Mouse primary osteoblasts were cultured with 10 mM of β-glycerophosphate in the presence or absence of 10^{-8} M of PMP22 for 3 weeks. Mineralization was assessed by Alizarin Red staining. Data represent the mean ± SEM (n = 5 in each group). **P < 0.05 (Mann-Whitney *U* test).

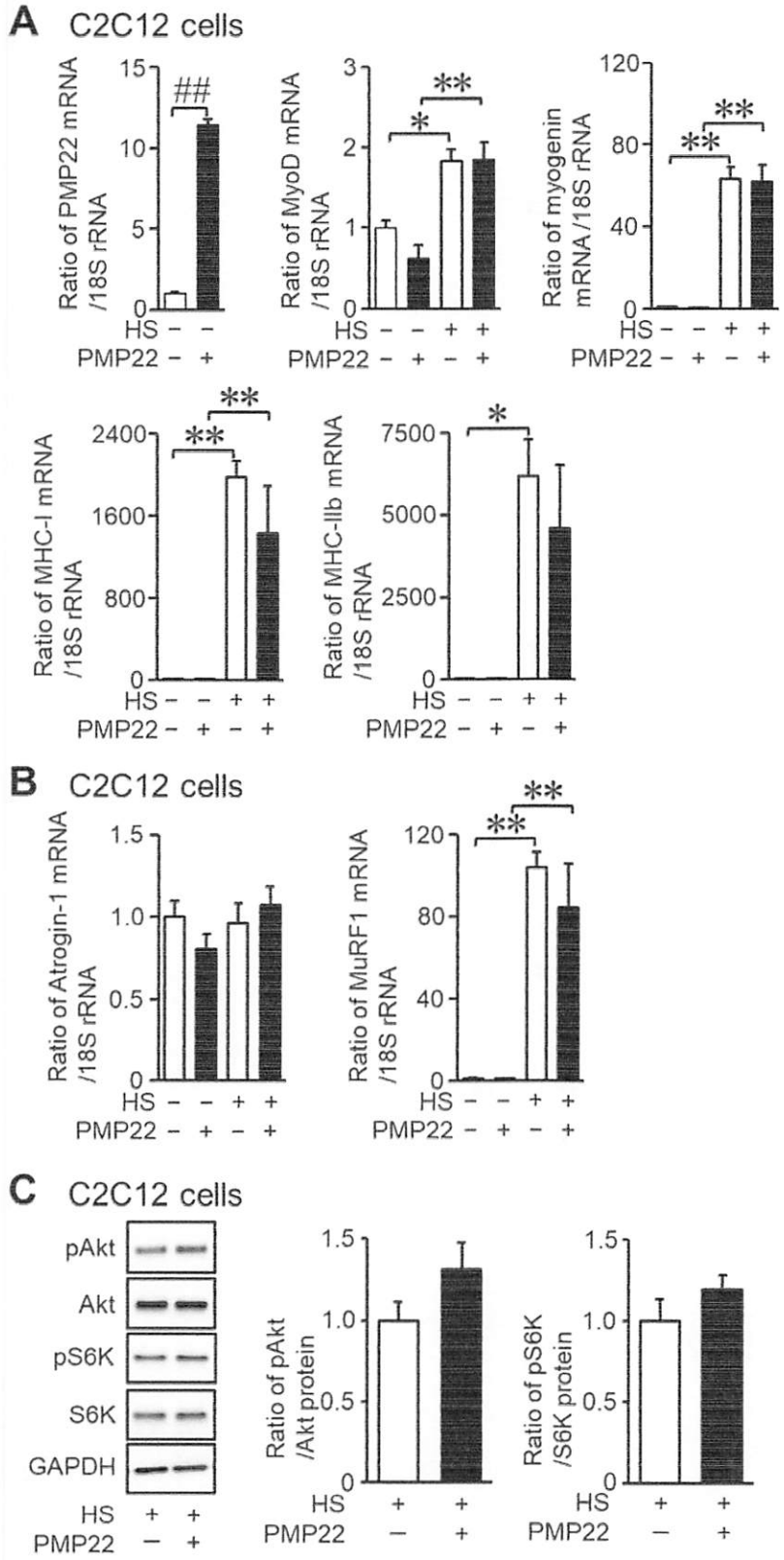

Figure 5 Effects of the transient expression of PMP22 on C2C12 cells. (A, B) Total RNA was extracted from C2C12 cells transfected with PMP22 cDNA or an empty vector in the presence or absence of horse serum for 5 days. A real-time PCR analysis of PMP22, MyoD, myogenin, MHC-I, MHC-IIb, atrogin-1, MuRF1 and 18S rRNA was performed. Data represent the mean ± SEM (n = 5 in each group). *P < 0.05, **P < 0.01 (Tukey-Kramer test). ##P < 0.01 (Mann-Whitney *U* test). (C) Total protein was extracted from C2C12 cells

transfected with PMP22 cDNA or an empty vector in the presence of horse serum for 5 days. Western blot analyses of phosphorylated Akt (pAkt), Akt, phosphorylated p70 S6 kinase (pS6K), S6K and GAPDH were performed. Data represent the mean ± SEM (n = 4 in each group).

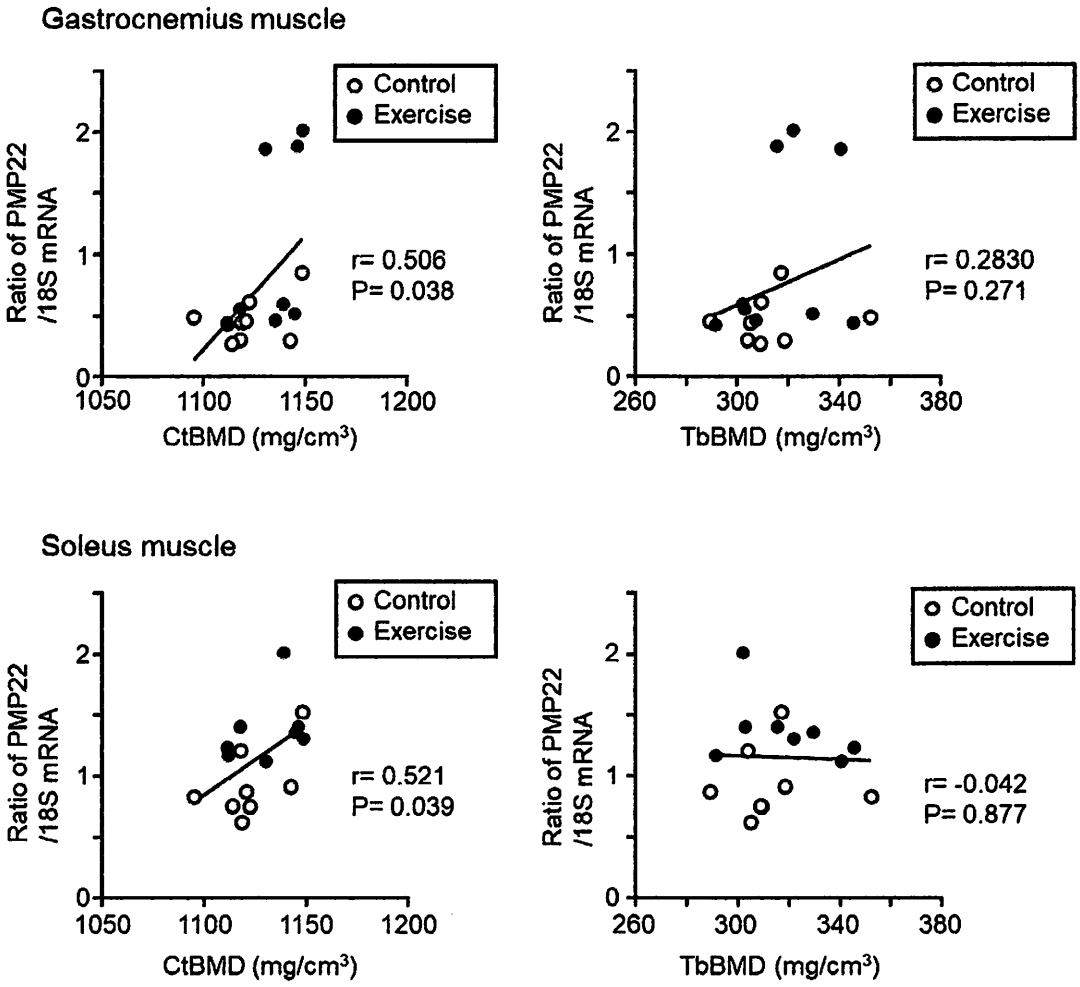

Figure 6 Relationships between PMP22 expression in gastrocnemius muscles and BMD in mice. A simple regression analysis was performed on PMP22 mRNA levels in the gastrocnemius and soleus muscles and cortical BMD (CtBMD) or trabecular BMD (TbBMD) in control and exercise mice Data represent 8 mice in each group.

3.6 Relationships between the expression of PMP22 in muscle and BMD

We examined the relationship between PMP22 expression in the gastrocnemius and soleus muscles and BMD at the femurs of mice using a simple regression analyses. As shown in Fig.

6, PMP22 mRNA levels in the gastrocnemius and soleus muscles were positively correlated with cortical BMD, but not trabecular BMD, at the femurs of mice with or without chronic exercise.

4. Discussion

PMP22, also known as CMT1, GAS3, PASI1, SR13 and HNPP, is a protein with 160 amino acids and a molecular weight of 22 kDa (Ashki et al., 2015). Subcellular localization database suggests that PMP22 is detected in extracellular space, nucleus and mitochondria as well as strong expression in plasma membrane (Developed by Janos Binder et al. from the Novo Nordisk Foundation Center for Protein Research (CPR), the Luxembourg Centre for Systems Biomedicine (LCSB), and the Commonwealth Scientific and Industrial Research Organisation (CSIRO).) Its expression has been detected in various tissues, predominantly in the peripheral nervous system, small intestine and placenta (Ashki et al., 2015). PMP22 is clinically known as a gene that is related to the pathogenesis of Charcot-Marie-Tooth disease and hereditary neuropathy with liability to pressure palsies (Li et al., 2013). PMP22 has a number of cellular functions, such as peripheral myelin formation, cell-cell interactions, cell growth and peroxisomal biogenesis (Ashki et al., 2015). Furthermore, the expression of PMP22 was shown to be reduced during the progression of lung cancer in an animal study (Ashki et al., 2015). In contrast, other studies suggested the amplification of PMP22 transcripts in cancers (van Dartel et al., 2002). PMP22 promoted the invasion ability of osteosarcoma cells partly through ERK1/2 and p38MAPK (Liu and Chen, 2015). In that study, PMP22 also appeared to enhance the migration, and colony formation of osteosarcoma. However, there have been no reports

available on the role of PMP22 in skeletal muscle and bone.

The present results showed that PMP22 suppressed M-CSF and RANKL-induced increases in osteoclast formation from mouse bone marrow cells. Moreover, PMP22 significantly reduced the increases in the expression of TRAP, cathepsin K, DC-STAMP and NFATc1 by M-CSF and RANKL in these cells, but significantly attenuated M-CSF and RANKL-induced decreases in the expression of MafB and IRF-8. Collectively, these results suggest that PMP22 suppresses osteoclast formation, which might lead to the suppression of bone resorption and increase in bone mass. We previously reported that chronic exercise attenuated decreases in trabecular and cortical BMD at the femurs following ovariectomy (Kawao et al., 2021). A simple regression analysis of samples from the same mice showed that the expression of PMP22 in the gastrocnemius and soleus muscles was positively related to cortical BMD at the femurs in the present study. Taken together, our data suggest that chronic exercise elevates secretion of PMP22 as a myokine linking muscle to bone. However, the results of the simple regression analysis revealed that the relationship between PMP22 expression in the gastrocnemius and soleus muscles and trabecular BMD at the femurs was not statistically significant. We therefore speculate that the effects of PMP22 might be dominant for the cortical bone, but not trabecular bone.

The RANKL/OPG system is a crucial mediator of the effects of osteotropic factors, such as parathyroid hormone and inflammatory cytokines, on bone resorption (Udagawa et al., 2021). However, PMP22 enhanced the expression of RANKL and increased the ratio of RANKL/OPG in mouse osteoblasts in the present study, suggesting that the effects of PMP22 on osteoclast formation were independent of the RANKL/OPG system. Some counteracting factors may

inhibit the effects of PMP22 on RANKL. Previous studies revealed that mitochondrial biogenesis is involved in osteoclast formation (Ishii et al., 2009; Lemma et al., 2016). We herein showed that PMP22 reduced OCR and expression of PGC1β in mouse bone marrow cells. These results suggest the possibility that PMP22 might attenuate osteoclast formation partly through a decrease in mitochondrial biogenesis in mouse bone marrow cells. A previous study demonstrated that the activation of NF-κB, ERK1/2 and p38 MAPK signaling induced an increase in NFATc1, which promoted the osteoclast formation (Koga et al., 2019). Liu and Chen showed that the overexpression of PMP22 enhanced the migration and invasion of osteosarcoma cells partly through the activation of ERK1/2 and p38 MAPK (Liu and Chen, 2015). In the present study, PMP22 suppressed the phosphorylation of ERK1/2 and the NF-κB p65 subunit, but enhanced that of p38 MAPK in mouse bone marrow cells. These results suggest that PMP22 might suppress osteoclast formation partly through the inhibition of ERK1/2 and NF-κB signaling in mouse bone marrow cells. Further studies are needed to elucidate the molecular mechanisms by which PMP22 suppresses osteoclast formation.

Regarding the effects of PMP22 on osteoblasts, PMP22 inhibited the expression of osteoblast differentiation-related factors, ALP activity and mineralization in mouse primary osteoblast cultures in the present study; however, it did not affect muscle mass-related phenotypes, such as muscle differentiation and muscle protein synthesis/degradation-related pathways in mouse muscle C2C12 cells. These results suggest that PMP22 negatively affects the osteoblast phenotype related to bone formation in mice. Since the simple regression analysis showed that the expression of PMP22 in the gastrocnemius and soleus muscles were positively related to cortical BMD at the femurs, the effects of PMP22 on osteoblasts appeared to be minor

compared to those effects on osteoclast formation, which might not induce an increase in BMD. We speculated that PMP22-suppressed bone resorption might overcome osteoblastic bone formation reduced by PMP22, then leading to an increase in bone mass by a positive balance of bone turnover in the way similar to the BMD increase observed in low turnover bone, such as hypoparathyroidism. However, how the effects of PMP22 on osteoblasts and osteoclasts *in vitro* reflect bone metabolism in vivo has still remained unknown in the present study.

The present study showed that chronic exercise significantly enhanced PMP22 expression in the gastrocnemius and soleus muscles of mice, but not in the femurs, WAT, kidneys or liver. These results suggest that PMP22 might be an exercise-induced myokine similar to irisin in mice. The effects of exercise on muscle and bone include increases in mechanical stress, sympathetic nerve activity, stress responses and blood supply. Since mechanical unloading with SNX significantly reduced the expression of PMP22 in the soleus muscles of mice and it seemed to reduce PMP22 expression in the gastrocnemius muscles without statistical significance, mechanical stress might partly explain the effects of chronic exercise on PMP22 expression in skeletal muscles. Alternatively, a mechanism other than mechanical stress may be contributing to the effects of chronic exercise on PMP22 expression in the skeletal muscles of mice.

Exercise therapy is essential for the prevention of osteoporosis and subsequent fragility fractures as well as successful drug therapy for osteoporosis. Although a follow-up of the physical status and exercise are important for the clinical care of osteoporotic patients, there are currently no effective biomarkers for exercise and physical activity. The present results raised the possibility that PMP22 might be a novel myokine linking muscle to bone in response to

chronic exercise in mice. Therefore, PMP22 may be expected to be an exercise biomarker for the prevention and treatment of osteoporosis. Although osteoporosis is age-related disease, we used young mice in the present study, which might limit the physiological relevance of our data.

In conclusion, we identified PMP22 as a novel myokine induced by chronic exercise for 8 weeks in mice from an RNA-seq analysis of skeletal muscles. We are the first to report that PMP22 suppresses osteoclast formation and the osteoblast phenotype *in vitro*. The PMP22-induced inhibition of bone resorption might lead to an improvement by exercise on BMD decreased by ovariectomy in mice.

Acknowledgments

This study was partly supported by a grant from All-Kindai University support project against COVID-19 to N.K., Grants-in-Aid for Scientific Research (C:20K09514) to H.K. and (C: 19K07310) to N.K., and a Grant-in-Aid for Scientific Research on Innovative Areas (grant number 15H05935, "Living in Space") to H.K. from the Ministry of Education, Culture, Sports, Science, and Technology of Japan.

Disclosure

The authors declare that they have no conflicts of interest with the contents of this article.

Data availability

The data sets used and/or analyzed during the current study are available from the corresponding author on reasonable request.

Author contributions

M.K., N.K. and H.K. contributed to the conception and design of the research. M.K. N.K., M.M., Y.T., M.I., Y.K., Y.T., Y.M. and T.O. performed experiments. M.K. analyzed the data. M.K., N.K. and H.K. interpreted the results of the experiments. M.K. prepared the figures. M.K. drafted the manuscript. M.K. and H.K. edited and revised the manuscript. All authors approved the final version of the manuscript.

References

Ashki N, Gordon L, Wadehra M. (2015). Review of the GAS3 family of proteins and their relevance to cancer. *Crit Rev Oncog* 20:435-447.

Baron R, Kneissel M. (2013). WNT signaling in bone homeostasis and disease: from human mutations to treatments. *Nat Med* 19:179-192.

Batra N, Burra S, Siller-Jackson AJ, Gu S, Xia X, Weber GF, DeSimone D, Bonewald LF, Lafer EM, Sprague E, Schwartz MA, Jiang JX. (2012). Mechanical stress-activated integrin α5β1 induces opening of connexin 43 hemichannels. *Proc Natl Acad Sci U S A* 109:3359-3364.

Gilchrist CL, Leddy HA, Kaye L, Case ND, Rothenberg KE, Little D, Liedtke W, Hoffman BD, Guilak F. (2019). TRPV4-mediated calcium signaling in mesenchymal stem cells regulates aligned collagen matrix formation and vinculin tension. *Proc Natl Acad Sci U S A* 116:1992-1997.

Ishii KA, Fumoto T, Iwai K, Takeshita S, Ito M, Shimohata N, Aburatani H, Taketani S, Lelliott CJ, Vidal-Puig A, Ikeda K. (2009). Coordination of PGC-1β and iron uptake in mitochondrial biogenesis and osteoclast activation. *Nat Med* 15:259-266.

Kaji H. (2013). Linkage between muscle and bone: common catabolic signals resulting in osteoporosis and sarcopenia. *Curr Opin Clin Nutr Metab Care* 16:272-277.

Kaji H. (2016). Effects of myokines on bone. *Bonekey Rep* 5:826.

Kawao N, Iemura S, Kawaguchi M, Mizukami Y, Takafuji Y, Kaji H. (2021). Role of

irisin in effects of chronic exercise on muscle and bone in ovariectomized mice. *J Bone Miner Metab* 39:547-557.

Kawao N, Kaji H. (2015). Interactions between muscle tissues and bone metabolism. *J Cell Biochem* 116:687-695.

Kawao N, Morita H, Iemura S, Ishida M, Kaji H. (2020a). Roles of Dkk2 in the linkage from muscle to bone during mechanical unloading in mice. *Int J Mol Sci* 21:2547.

Kawao N, Morita H, Obata K, Tatsumi K, Kaji H. (2018a). Role of follistatin in muscle and bone alterations induced by gravity change in mice. *J Cell Physiol* 233:1191-1201.

Kawao N, Moritake A, Tatsumi K, Kaji H. (2018b). Roles of irisin in the linkage from muscle to bone during mechanical unloading in mice. *Calcif Tissue Int* 103:24-34.

Kawao N, Takafuji Y, Ishida M, Okumoto K, Morita H, Muratani M, Kaji H. (2020b). Roles of the vestibular system in obesity and impaired glucose metabolism in high-fat diet-fed mice. *PLoS One* 15:e0228685.

Kawao N, Tamura Y, Okumoto K, Yano M, Okada K, Matsuo O, Kaji H. (2013). Plasminogen plays a crucial role in bone repair. *J Bone Miner Res* 28:1561-1574.

Kemmler W, Shojaa M, Kohl M, von Stengel S. (2020). Effects of different types of exercise on bone mineral density in postmenopausal women: A systematic review and meta-analysis. *Calcif Tissue Int* 107:409-439.

Koga Y, Tsurumaki H, Aoki-Saito H, Sato M, Yatomi M, Takehara K, Hisada T. (2019). Roles of cyclic AMP response element binding activation in the ERK1/2 and p38

MAPK signalling pathway in central nervous system, cardiovascular system, osteoclast differentiation and mucin and cytokine production. *Int J Mol Sci* 20:1346.

Lemma S, Sboarina M, Porporato PE, Zini N, Sonveaux P, Di Pompo G, Baldini N, Avnet S. (2016). Energy metabolism in osteoclast formation and activity. *Int J Biochem Cell Biol* 79:168-180.

Li J, Parker B, Martyn C, Natarajan C, Guo J. (2013). The PMP22 gene and its related diseases. *Mol Neurobiol* 47:673-698.

Liu S, Chen Z. (2015). The functional role of PMP22 gene in the proliferation and invasion of osteosarcoma. *Med Sci Monit* 21:1976-1982.

Schnyder S, Handschin C. (2015). Skeletal muscle as an endocrine organ: PGC-1α, myokines and exercise. *Bone* 80:115-125.

Shimoide T, Kawao N, Morita H, Ishida M, Takafuji Y, Kaji H. (2020). Roles of olfactomedin 1 in muscle and bone alterations induced by gravity change in mice. *Calcif Tissue Int* 107:180-190.

Smith JK. (2018). Exercise, obesity and CNS control of metabolic homeostasis: A review. *Front Physiol* 9:574.

Takafuji Y, Tatsumi K, Ishida M, Kawao N, Okada K, Kaji H. (2020). Extracellular vesicles secreted from mouse muscle cells suppress osteoclast formation: Roles of mitochondrial energy metabolism. *Bone* 134:115298.

Takafuji Y, Tatsumi K, Kawao N, Okada K, Muratani M, Kaji H. (2021). MicroRNA-

196a-5p in extracellular vesicles secreted from myoblasts suppresses osteoclast-like cell formation in mouse cells. *Calcif Tissue Int* 108:364-376.

Tamura Y, Kawao N, Yano M, Okada K, Matsuo O, Kaji H. (2014). Plasminogen activator inhibitor-1 deficiency ameliorates insulin resistance and hyperlipidemia but not bone loss in obese female mice. *Endocrinology* 155:1708-1717.

Udagawa N, Koide M, Nakamura M, Nakamichi Y, Yamashita T, Uehara S, Kobayashi Y, Furuya Y, Yasuda H, Fukuda C, Tsuda E. (2021). Osteoclast differentiation by RANKL and OPG signaling pathways. *J Bone Miner Metab* 39:19-26.

van Dartel M, Cornelissen PW, Redeker S, Tarkkanen M, Knuutila S, Hogendoorn PC, Westerveld A, Gomes I, Bras J, Hulsebos TJ. (2002). Amplification of 17p11.2 approximately p12, including PMP22, TOP3A, and MAPK7, in high-grade osteosarcoma. *Cancer Genet Cytogenet* 139:91-96.

Wallace BA, Cumming RG. (2000). Systematic review of randomized trials of the effect of exercise on bone mass in pre- and postmenopausal women. *Calcif Tissue Int* 67:10-18.

Wang L, You X, Lotinun S, Zhang L, Wu N, Zou W. (2020). Mechanical sensing protein PIEZO1 regulates bone homeostasis via osteoblast-osteoclast crosstalk. *Nat Commun* 11:282.

Wang N, Liu Y, Ma Y, Wen D. (2017). High-intensity interval versus moderate-intensity continuous training: Superior metabolic benefits in diet-induced obesity mice. *Life Sci* 191:122-131.

Zeng R, Faccio R, Novack DV. (2015). Alternative NF-κB regulates RANKL-induced osteoclast differentiation and mitochondrial biogenesis via independent mechanisms. *J Bone Miner Res* 30:2287-2299.